Transcrystalline regions in the vicinity of nanofillers in polyamide-6

Dasari, Aravind; Yu, Zhong-Zhen; Mai, Yiu-Wing

2007

Dasari, A., Yu, Z.-Z., & Mai, Y.-W. (2007). Transcrystalline regions in the vicinity of nanofillers in polyamide-6. Macromolecules, 40(1), 123-130.

https://hdl.handle.net/10356/101501

https://doi.org/10.1021/ma0621122

On Trans-Crystalline Regions in the Vicinity of Nano-Fillers in Polyamide 6

Aravind Dasari, Zhong-Zhen Yu and Yiu-Wing Mai

Centre for Advanced Materials Technology (CAMT)

School of Aerospace, Mechanical and Mechatronic Engineering (J07)

The University of Sydney, Sydney, NSW 2006, Australia

Received date

Full Paper

Abstract

The presence of preferential organization of lamellar regions in the vicinity of soft (maleic anhydride grafted polyethylene-octene copolymer, POE-g-MA) and rigid (clay) nano-fillers and how these interfaces or ligament regions between the nano-additives and a polymer, polyamide 6, contribute towards the toughening processes were studied. The preferential lamellar orientation was observed only in the core region of the injection molded polymer nanocomposites; while in other regions flow-induced crystallization was the controlling factor. In the case of soft-fillers, it was shown that the orientation of trans-crystalline lamellae along the tensile direction to promote shear yielding is a complex process, but it is not a predominant factor controlling the total toughness of the polymer blend, which is the sum of all the deformation processes occurring in all the regions (i.e., surface, intermediate, and core) of the injection molded samples. For rigid clay systems, delamination of the clay layers occurred and resulted in only a slight increase of the toughness. Hence, it was suggested that without extensive matrix shear yielding activated by full debonding of the clay/matrix interfaces, large improvements in toughness cannot be realized.

Introduction

Changing the processing conditions, e.g. combination of shear and extensional flow, and/or addition of fillers, generally influence the spatial organization and alignment of crystallites in semi-crystalline polymers and thus may affect the material properties such as strength, hardness, toughness and transparency.[1-6] In neat polymers, the negligible shear in the center of an injection-molded bar and the presence of intense shear near the surface are shown to produce different spatial organizations of the crystalline lamellae.[6-8] With the addition of fillers, particularly fibers, many studies have shown that they act as heterogeneous nucleating agents and initiate crystallization along the interface.[9-13] However, the essential pre-requisite for this to happen is the presence of a high density of active nuclei on the filler surface. These nuclei hinder the lateral extension of spherulites and force their growth normal to the fiber surfaces resulting in columnar crystalline layers, called trans-crystalline layers, with some finite thickness.[14,15] The nucleation and trans-crystalline growth is also reported to be system-dependent, that is, affected by the topography of the filler, the mismatch of thermal expansion coefficients between filler and matrix, thermal conductivity and surface energy of filler, chemical composition of filler surface, and stress-induced crystallization by local flow. Though the exact mechanisms of the trans-crystalline growth are still not clear, it is commonly agreed that extensive heterogeneous nucleation of polymer melts at high energy surfaces generates trans-crystalline layers in the interfacial region if sufficient time is allowed for the polymer melt to achieve extensive and intimate contact with the filler. Therefore, the spherulites disappear and the trans-crystals appear at the filler surface and become dominant when the filler surface energy increases. Cho *et al.*[16] compared the effect of substrate (silicon) surface energy on the trans-crystalline growth at the interface of semi-crystalline isotactic polypropylene by treating the substrate with various silane coupling agents so as to change the surface energy. They showed that with a high surface energy substrate, the trans-crystalline region is very thick when compared to a low surface energy substrate. However, it is still unclear whether the trans-crystalline layers are beneficial for shear stress transfer at the interface, thereby improving the mechanical properties; or if they have a negative or negligible effect on the ultimate mechanical properties.

The existing knowledge-base is even worse for the case of (rigid or soft) nano-fillers. It is not fully understood (experimentally and/or physically), even after decades of studies on semi-crystalline polymer nanocomposites, how the presence of the trans-crystalline layers and the interfaces or ligament regions between nano-additives and a polymer affect the mechanical properties of the nanocomposites, despite some theories and models have been proposed. For example, with soft elastomeric additives, Muratoglu *et al.*[5] proposed that in the inter-particle regions of closely spaced particles, nylon lamellae are arranged close to each other and perpendicular to the rubber-matrix interface. Therefore, the hydrogen-bonded planes of low slip resistance are aligned parallel to these interfaces. Consequently, under an external applied load, upon cavitation of the rubber particles, the local deformation will be easily initiated on these planes, and eventually allows deformation to large strains without initiating any critical fracture process, hence enhancing the toughness. Generally, the influence of the interface is negligible when the filler is amorphous. However, many studies[17,18] have shown that even amorphous substrates can induce an ordered crystalline growth in the crystallizing matrix including the above-mentioned work.[5] A similar morphology is reported in polymers that are crystallized on planar substrates (rubber and calcite) suggesting that the crystallization behavior near an incoherent (or dissimilar) interface is different from that occurring in the bulk and is independent of the nature of the substrate, be that amorphous or crystalline.[19] Polyethylene has been demonstrated to crystallize preferentially in the interfacial zones with the lamella oriented edge-on against the substrate and with a strong preferred orientation of the crystallographic (100) planes lying parallel to the interface. This was attributed to the accelerated secondary nucleation on these lamellae. These similar oriented crystallization behaviors in different material systems suggest that this type of crystallization near dissimilar interfaces is common in semi-crystalline polymers for a wide variety of interface types. In contrast, Corte *et al.*[4] have recently shown that in injection molded nylon 12/ethylene-propylene rubber (EPR) system, the crystalline lamellae are aligned in the same direction over tens of microns pointing to the absence of any trans-crystallization zone in the vicinity of the amorphous rubber fillers. However, it is important to realize the effects of flow-induced crystallization when considering the preferred orientation of lamellae in the vicinity of particles. Corte *et al.*[4] examined the intermediate regions of the injection molded bar, that is, in-between surface and core, where the influence of shear exists and so the lamellae are aligned normal

to the flow direction consistent with the theories of flow-induced crystallization;[8] while Muratoglu *et al.*[5] investigated spin-coated thin films in order to remove any such shear-induced effects.

With rigid particles, especially clay, there were several attempts to understand the trans-crystallization behavior of polyamide induced by the presence of nano-clay. It has been shown that in an intercalated system polyamide lamellae are oriented perpendicular to the intercalated clay layers and the flow direction, extending over several microns.[3] Although the authors suggest this to be the trans-crystallization process, it raises a critical question whether the preferred orientation is a direct result of the presence of the clay layers or a combination of the presence of clay layers (acting as nucleation agents) and flow-induced crystallization. Based on the observations of Kim *et al.*[3] and assuming that the entire material to be trans-crystalline, Sheng *et al.*[20] included the effect of the trans-crystallized matrix layers to calculate the enhancement of the composite modulus using finite element simulation. They assumed that each particle has a trans-crystalline matrix layer of thickness ~50 nm on either side. While the trans-crystallization of the matrix does contribute to the enhancement of the overall composite modulus, however, this effect was found to be very minor in comparison with the 'composite-level' effects of stiff particles in the matrix.

In the present study, we focus mainly on some fundamental aspects so as to understand the preferred orientation of crystalline lamellae in the vicinity of soft (maleic anhydride grafted polyethylene-octene copolymer, POE-g-MA) and rigid (clay) nano-fillers in a polyamide 6 matrix and their role towards toughening.

Experimental Section

Materials and preparation: Polyamide 6 with a trade name of Akulon F 232-D was obtained from DSM Engineering Plastics (The Netherlands). Maleic anhydride grafted polyethylene-octene copolymer (POE-g-MA) with an MA content of 0.6 wt.% was purchased from Rui-Sheng Co. (Taiwan). Since it is well-established that the affinity of organoclay with matrix plays a dominant role in determining the extent of exfoliation, two types

of commercial organoclays were used to achieve exfoliated (Cloisite® 93A) and intercalated (Cloisite® 15A) nanocomposites. The alkyl ammonium surfactant used in Cloisite® 93A was methyl, dihydrogenatedtallow ammonium, while dimethyl, dihydrogenatedtallow, quaternary ammonium was used in Cloisite® 15A. The cation exchange capacity and %wt. loss on ignition were about 90 mequiv/100 g and 40% for Cloisite® 93A and 125 mequiv/100 g and 43% for Cloisite® 15A, respectively. Both organoclays were obtained from Southern Clay Products Inc. (USA) via Jim Chambers & Associates (Australia).

Polyamide 6 pellets, POE-g-MA pellets, and the two types of organoclay were oven-dried at 85^{o}C for 24 h. Then, the desired proportions of the ingredients were mixed and melt compounded in a Werner & Pfleiderer ZSK-30 twin-screw extruder (L/D = 30, L = 0.88 m). Extrusion was performed within the temperature range of 210-245^{o}C and a screw speed of 300 rpm. Subsequently, the extruded pellets were oven-dried and molded into tensile and rectangular bars using a Boy Dipronic 22S injection molding machine with the barrel and mold temperatures maintained at 235^{o}C and 60^{o}C, respectively. Binary polyamide 6/organoclay nanocomposites (90/10) and binary polyamide 6/POE-g-MA blends (70/30 and 90/10) along with neat polyamide 6 were prepared using the above-mentioned conditions. The notched Izod impact energies (kJ/m^2) of the materials were evaluated in an ITR-2000 instrumented impact tester per ASTM D256 on the injection molded rectangular bars and are listed in Table 1. In the blends, it is evident that with increasing POE-g-MA content, the fracture mode changed from brittle to ductile. Significant toughening effect is achieved at 30 wt.% POE-g-MA. All these tests were conducted at ambient temperature (20-25°C) and an average value of five repeated tests was reported for each composition.

Morphology observations: To investigate the preferred orientation of lamellae in the vicinity of nanoparticles, ultra-thin sections of ~60-90 nm in thickness were cryogenically cut with a diamond knife in liquid nitrogen environment at –100^{o}C using a Leica Ultracut S microtome. Sections were collected on formvar/carbon coated 400-mesh copper grids. Subsequently, to reveal the crystalline lamellae, sections were stained with an aqueous solution of phosphotungstic acid (H_3PO_4.12 WO_3) and benzyl alcohol ($C_6H_5CH_2OH$) according to the method

described by Martinez-Salazar and Cannon.[21] They were then observed using a Philips CM12 transmission electron microscope (TEM) at an accelerating voltage of 120 kV.

Table 1. Notched Izod impact energy of all studied materials.

Material	Notched Izod Impact Energy, kJ/m^2
Neat Polyamide 6	7.1 ± 0.2
Polyamide 6/POE-g-MA Blend (90/10)	13.0 ± 0.1
Polyamide 6/POE-g-MA Blend (70/30)	104.4 ± 1.0
Polyamide 6/clay Exfoliated Nanocomposite (90/10)	3.2 ± 0.1
Polyamide 6/clay Intercalated Nanocomposite (90/10)	4.3 ± 0.01

Results and Discussion

Lamellar organization in nylon 6/POE-g-MA blends: Figures 1a and 1(b, c) show typical TEM micrographs in the core region (along a plane parallel to the flow direction) of an injection molded polyamide 6/POE-g-MA binary blend at 10 and 30 wt.% of POE-g-MA, respectively. At 10 wt.% elastomeric phase, the prevalence of lamellae impinging on particle interfaces is apparent for all the particles (indicated by the arrows), which points to the existence of preferentially oriented lamellar zone (each around 10-30 nm) in the vicinity of the soft particles; while in the rest of the matrix, the lamellae are randomly oriented. This morphology confirms that dissimilar interfaces may promote oriented crystallization in the absence of any external stress field. The crystalline lamellae appear bright and are separated by thin and dark amorphous layers due to the negative staining. However, since the inter-particle distances are large at this content of elastomeric phase, only lamellae radiating from the particles are seen and occasionally where adjacent particles are intimately near to each other, the inter-particle regions of these particles show a different morphology whereby the lamellae appear to be "interpenetrating" caused by the fact that they are very closely spaced. This behavior is more obvious at higher percentages of POE-g-MA (30 wt.%, Figures 1b and 1c for low and high magnifications) where the inter-particle distances are

very small. The close organization of the lamellae in these regions is marked with dotted circles. As mentioned earlier, Muratoglu *et al.*[5] suggested that this morphology if percolates throughout the entire blend, the overall plastic resistance is reduced hence initiating a high toughness response. Compared to the present study where transcrystalline regions are observed in the core of an injection molded bar where the influence of shear flow is negligible, Corte *et al.*[4] have, however, shown that there are no transcrystalline layers in nylon 12/EPR blend in the vicinity of EPR particles under the influence of shear. To confirm these results, we also took TEM images close to the surface of the injection molded bar.

In Figures 1d and 1e, TEM micrographs of the injection molded polyamide 6/POE-g-MA binary blends taken along a plane parallel to the flow direction (close to the surface) at 10 and 30 wt.% of POE-g-MA, respectively, are shown. There are no preferentially oriented crystalline lamellae around the particles at all contents of POE-g-MA as in the core region (Figures 1a-c). Additionally, even when the inter-particle spacing is smaller (at 30 wt.% of POE-g-MA, Figure 1e), no crystalline lamellae are organized closely. It is interesting to see that the crystalline organization in the vicinity of the particles is not dominated by the particles, but controlled by the processing conditions, in particular, the flow direction (indicated by double-headed arrows, identified from the shape of elongated particles in the region). It is evident that most of the lamellae are extended in a direction almost normal to the flow direction for several hundreds of nanometers in a manner similar to the study of Corte *et al.*[4] Similar observations were also reported in other systems. Lagasse and Maxwell[22] showed that shear-induced crystallization of propylene polymers was unaffected by the presence of either a carbon black additive or a heterogeneous nucleating agent. Keller[23] found that primary nucleation occurred in melt-drawn polyethylene along a line or row normal to the draw-direction, which he called *row-nucleation*. The resulting crystals grew normally outward from this line.

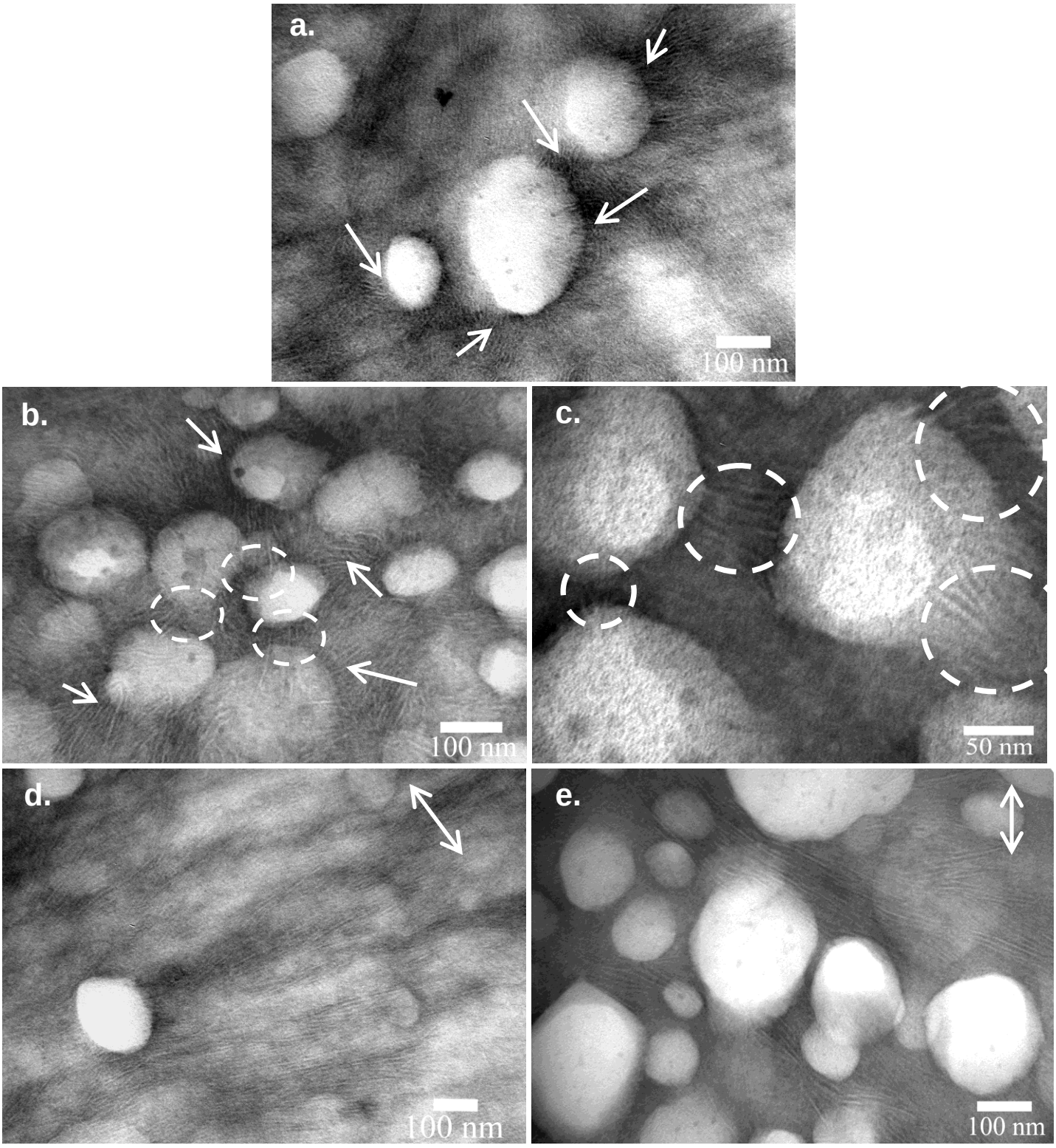

Figure 1. TEM micrographs taken in the core (a, b, c) and near-surface (d, e) regions of injection molded polyamide 6/POE-g-MA blends along a plane parallel to the flow direction for (a, d) 10 wt.% and (b, c, e) 30 wt.% showing the crystalline organization.

The above observations (Figure 1) indicate that in the injection molded samples, the structural organization of crystalline lamellae is very complex and is heavily influenced by shear-induced flow. In the surface regions subjected to high shear, flow-induced crystallization dominates; while in the core regions under negligible shear, crystalline organization is mainly controlled by the dispersed particles and form preferentially oriented lamellar zones. *This complex structural organization of lamellae in different zones of the bar will ultimately affect the toughening processes and total toughness value from the combined deformation of all these regions*. Considering this fact, the proposed model of Muratoglu *et al.*[5] (in which it was assumed that the entire blend is trans-crystalline) to elucidate the deformation and toughening mechanisms is only valid, if at all, in the core region of the injection molded bar not experiencing any shear flow.

Morphology changes during tensile straining: To clearly identify the role of preferred lamellar organizations, in particular, the closely-spaced lamellae in the inter-particle regions towards the toughening processes, uniaxial tensile test was conducted on polyamide 6/POE-g-MA (70/30) blend at a cross-head speed of 5 mm/min and subjected to a selected extension of 60% whence the material was uniformly stretched. Ultra-thin sections were cryo-microtomed from the core region along the plane parallel to the flow direction from uniformly stretched locations. TEM micrographs taken from this region are shown in Figure 2. The tensile stretching direction was identified from the shape of elongated particles/cavities in the region.

Before discussing TEM results, it is important to note that when a polymer/rubber blend is subjected to external loading, cavitation may occur when the hydrostatic stress component reaches a critical value.[24,25] In general, it is well-established that when the adhesion between rubber and matrix is strong enough, cavitation takes place inside the rubber particle due to the difference in Young's modulus and Poisson's ratio between the particle and matrix. In contrast, when the adhesion between rubber and matrix is relatively poor, interfacial debonding may occur. But, in the present case, the interfacial interaction between the POE-g-MA particles and polyamide 6 matrix is improved by *in-situ* formation of polyamide 6-co-POE-g-MA copolymer. Particle cavitation and void formation should relieve the plane strain constraint on the matrix material adjacent to the cavitated particles,

facilitating easy yielding of the lamellae in the closely-spaced particles. Since the yield stress depends on the degree of constraint,[26] cavitation of particles promotes shear yielding in the matrix ligaments. However, it is important to mention that depending on the level of compatibility of the dispersed additive with the surrounding phase and the concentration of stress, the criterion for cavitation of POE-g-MA particles varies from particle to particle, thus complicating the picture.

TEM micrograph (Figure 2a) shows large extents of rubber particle stretching and in a few locations, considerable amount of oriented lamellar regions (white arrows) along the tensile direction (double white arrows) within the uniformly strained section. In un-deformed condition, a large percentage of rubber particles are in the size range 100-150 nm (see for example, Figure 1b), although a broad range of size distribution is observed. While in the stretched condition, most of the particles are in the size range 230-300 nm or larger (measured along the long axis of stretched particles) indicating the extent of stretching (see for example, Figure 2a). Quantification of results was based on five TEM micrographs taken in the core region of injection molded polyamide 6/POE-g-MA blends along a plane parallel to the flow direction at different magnifications using a Soft Imaging Systems 'analySIS' software. Apart from the rubber particles, however, there are many locations where the lamellae are not oriented along the tensile direction, some of which are shown with black arrows. This indicates the complexity of this process and possible dependence on the cavitation of rubber particles to relieve the constraint on the matrix. At some locations, it also appears that the rubber particles have deformed and coalesced together to an extent that makes it difficult to identify precisely the closely-spaced lamellar organizations amongst them. Furthermore, as the rubber particles are not positively stained, it is difficult to identify whether cavitation has occurred or not. It should also be noted here that accurately staining POE elastomeric particles is difficult with the commonly used staining agents like RuO_4 or OsO_4; if an ultra-thin section of polyamide 6/POE blend is exposed to RuO_4 vapor, as the staining rates of polyamide and POE are very different, polyamide 6 will turn grey first while the POE particles remain white. However, if the particles are embedded in the matrix or lie on top of each other, bright regions may not always correspond to the cavitated particles and may lead to possible misinterpretations. To avoid all these confusions, ultra-thin sections

of the tensile strained sample were also checked in TEM before being negatively stained to identify if there are any voids. In Figure 2b, although voids (relating to cavitation of POE-g-MA particles) are clearly observed, it is apparent that not each and every elastomer particle has cavitated. This also supports the explanations given above and Figure 2a why only in some locations the closely-spaced lamellae orientate along the tensile direction, while at other locations, there is no orientation.

It is again essential to make a point that the preferred oriented layers are only found in the core region of the injection molded bar, which is a small region; but the total toughness of the polyamide 6/POE-g-MA blend is the sum of deformation processes in all regions (surface, intermediate and core) suggesting that the preferential alignment of lamellae in the inter-particle regions *may not be a predominant factor* controlling the toughness of the polymer blend. Moreover, for the polyamide 6/POE-g-MA (90/10) blend, under an external load, though some cavitation of the rubber particles has occurred, it still fails in quite brittle manner (Table 1) indicating that when the inter-particle distances are large, matrix shear-yielding cannot be effective and widespread.

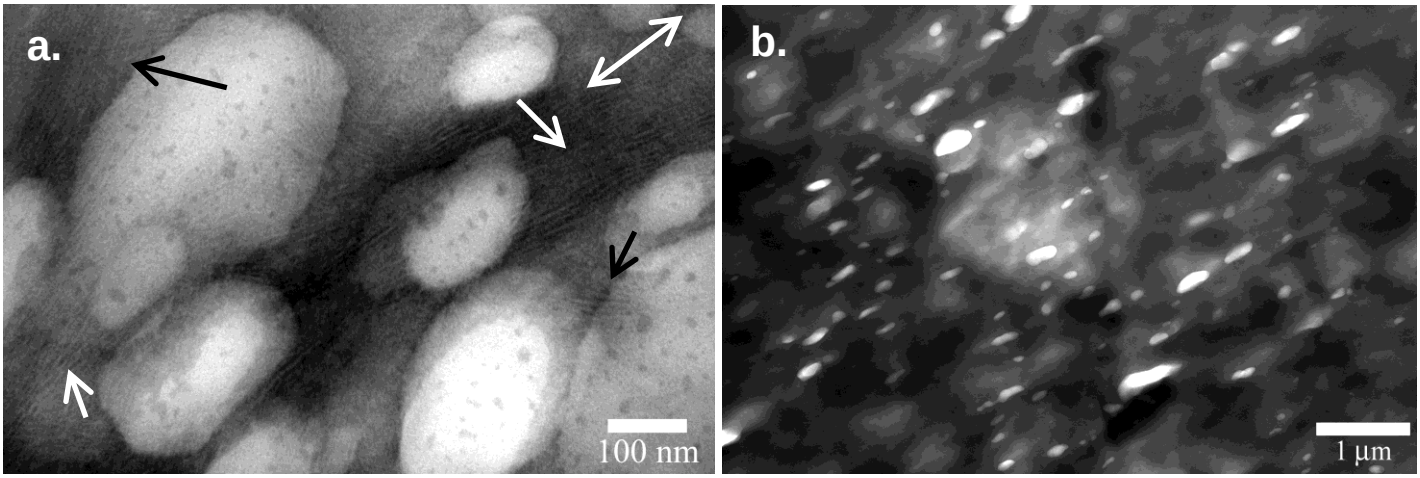

Figure 2. TEM micrographs showing the complexity of the process of lamellae orientation after tensile straining to an extension of 60%: (a) negatively stained to reveal the lamellae, and (b) without any staining to identify cavitation. Tensile direction is shown with double-headed arrows; white single arrows point to the oriented crystalline lamellae along tensile direction, while black arrows indicate the lamellae that are not oriented along the tensile direction.

Lamellar organization in polyamide 6/clay nanocomposites: Figure 3a shows TEM micrograph of the core region of injection molded polyamide 6/clay (90/10) nanocomposite taken along a plane perpendicular to the flow direction and negatively stained to reveal the crystalline organization. Clay layers are randomly and uniformly dispersed in the polymer matrix. It is also interesting to see that the crystalline lamellae are aligned perpendicular to the lateral interface (on both sides) of each clay layer and matrix, and appear closely organized to each other depending on the orientation of the clay layers. These trans-crystalline layers are around 30-40 nm (including both sides) for each clay layer and confirm that nucleation occurs at the silicate surface during crystallization of the polyamide matrix. It is also suggested previously that the ammonium cations at the ends of polyamide 6 molecules are bonded with the anionic sites on the silicate mono layers.[27] If polyamide molecules are densely bonded to a silicate monolayer, this nucleation results in the growth of lamellae normal to the silicate monolayer when they are not affected by an external stress field. In addition, TEM observations close to the surface of injection molded polyamide 6/organoclay (90/10) nanocomposite, where there are high shear stresses, reveal that the nano-clay layers are highly oriented in one particular direction; while the polyamide lamellae are oriented normal to that direction over the entire region (Figure 3b). This again suggests that in the near-surface region of injection molded bars, the lamellae organization is not controlled by the presence of fillers but is primarily determined by the flow-induced crystallization.

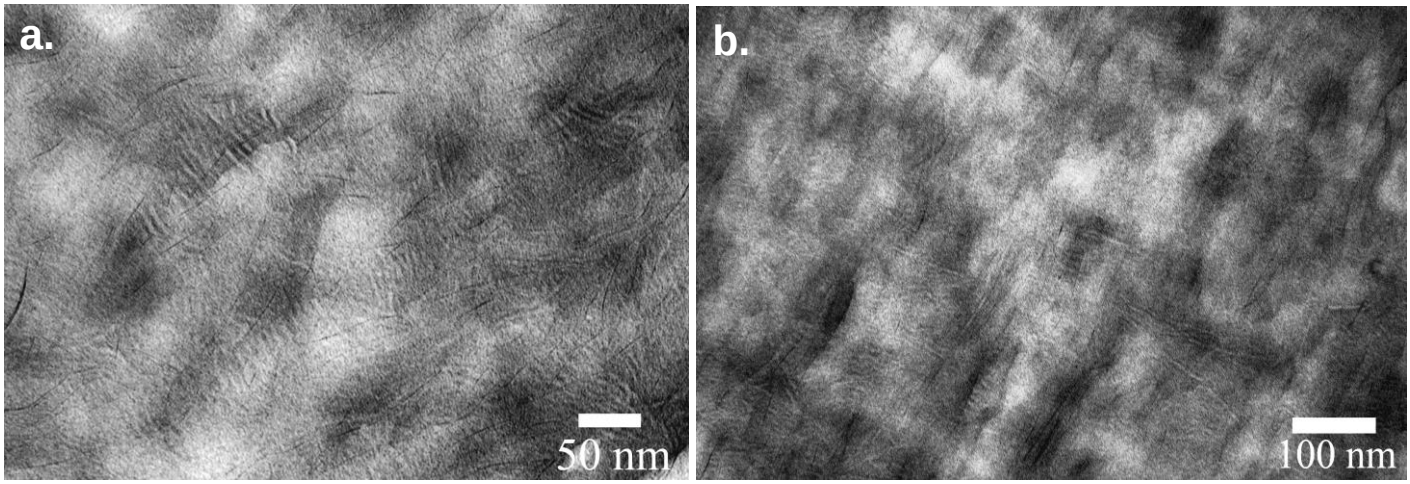

Figure 3. TEM micrographs taken in (a) core and (b) near-surface regions of injection molded polyamide 6/organoclay nanocomposite (90/10) along a plane normal to the flow direction showing the crystalline organization.

Morphology changes during tensile straining: Kim *et al.*[3] performed *in situ* tensile tests of intercalated polyamide-12 clay nanocomposites within an electron microscope and observed that the major deformation process in these materials was micro-void formation inside the stacked silicate layers. Since the clay interlayer strength is weaker than the clay/matrix interfacial strength, delamination or interlayer debonding of clay tactoids occurs. This phenomenon was reported in poly(vinylidene fluoride)/silicate nanocomposites[28] during tensile testing and also in other polymer/clay systems experiencing other modes of damage. For example, in polyamide 66/clay nanocomposites during nanoscratching (1 mN applied normal load and a sliding speed of 1 μm/s) submicron and nanocracks associated with the clay layers (formed between them) were observed up to 500 nm below the scratch track.[29] Depending on the orientation of intercalated clay structures, delamination in tensile mode of deformation can cause splitting, opening or sliding and any combination thereof of the high surface area clay layers.[3] It is important to note that unlike spherical nano-fillers, clay platelets due to their 2-D nanostructure exhibits significant orientation differences on any one plane varying from a fully disc shape to a fine layer. Due to its high aspect ratio, during injection molding into a tensile or rectangular bar, only translation motion of clay platelets is possible and rotational motion is generally negligible. So generally, along a plane parallel to the flow direction, large percentages of disc shaped particles are present. In the study of Kim *et al.*[3], the observations were made along this plane, which makes it difficult to identify those micro-voids formed by the real deformation processes and the presence of discs or those removed during the microtoming (which can be easily removed if microtomed along this plane). To avoid these confusions, in the present study, after tensile stretching to different extensions, the samples were microtomed along the plane normal to the flow direction.

With similar lamellae organization between clay layers as that between rubber particles, a pertinent question is why the notched Izod impact energy of exfoliated polyamide 6/clay nanocomposites is low (Table 1). Recall that rubber cavitation is a necessary condition for matrix shear yielding to impart high toughness to the polymer /rubber blends. Hence, it would seem that debonding at the polymer/clay interface is also a necessary condition for effective toughening in these polymer/clay nanocomposites so that shear yielding of large volumes of matrix material can be enhanced. When the sample is unloaded before reaching the tensile yield stress but beyond the

elastic limit, in the core region of exfoliated polyamide 6/clay nanocomposites, no debonding or delamination of the exfoliated, nano-scale dispersed, and high aspect ratio clay layers is observed (Figure 4a, here the matrix is not stained to clearly identify the fine delamination between clay layers). But when the sample is subjected to an extension corresponding to the tensile yield stress, submicron voids that are associated with clay layers are observed at some locations. A TEM micrograph exemplifying this behavior is shown in Figure 4b. It is clearly revealed that the submicron void is formed as a result of delamination of the clay layers. As most of the clay layers are exfoliated and dispersed at nano-scale, submicron to nano-sized voids are associated with those layers where two or more layers are stacked together due to the weak interaction between these stacked silicate layers. However, no debonding of clay layers from the matrix is observed due to the strong tethering junctions. When the sample is stretched to an extension of 60%, just before fracture, delamination is observed at more locations, but still not on a massive scale (Figure 4c). It is important to note that no deformation structure representing debonding of clay layers from the matrix is present even at this stage, indicating that the constraint on the polymer has not been relaxed. This is understandable if the trans-crystalline regions in the vicinity of the delaminated nano-clay layers are revealed. An illustration of this is shown in Figure 4d, a high magnification TEM micrograph taken at this location, which shows the clear persistence of trans-crystalline regions (pointed with arrows) in the vicinity of even the delaminated layers.

Delamination will result in an increase of interlayer distance (movements of the clay layers), hence dissipating energy in deforming the polymer inside the intra-gallery and the trans-crystalline lamellae that are firmly bonded to the outermost surfaces of the clay particle. As the extent of delamination is very limited in this case and no debonding of clay layers from matrix is observed, which are necessary for creating free volume in the matrix, the material failed in a brittle manner with a low impact energy value. In contrast, in an intercalated polyamide 6/clay nanocomposite, in a manner similar to other studies[3,28], large scale delamination of clay layers resulting in the formation of submicron voids are observed. But no debonding of clay layers from the matrix can be seen even in this case at all the locations investigated. High magnification TEM micrographs showing the delamination of intercalated clay layers (without staining the matrix) taken from the core region along the plane

normal to the flow direction upon unloading to different extensions (corresponding to tensile yield stress and to a selected extension of 60%) are shown in Figures 5a and 5b and an example showing the effect of delamination of clay layers on the trans-crystalline regions in their vicinity is shown in Figure 5c (pointed with arrows). Due to the large scale delamination of intercalated clay layers and the formation of submicron voids, the increase in inter-layer distance is large. Thus, the toughness is increased, albeit moderately, compared to the exfoliated polyamide 6/clay nanocomposite (Table 1). However, it is thought that without extensive matrix shear yielding activated by full debonding of the clay/matrix interfaces, similar to the cavitation of POE-g-MA rubber, large improvement in toughness in semi-crystalline polymer/rigid clay nanocomposites will not be realized.

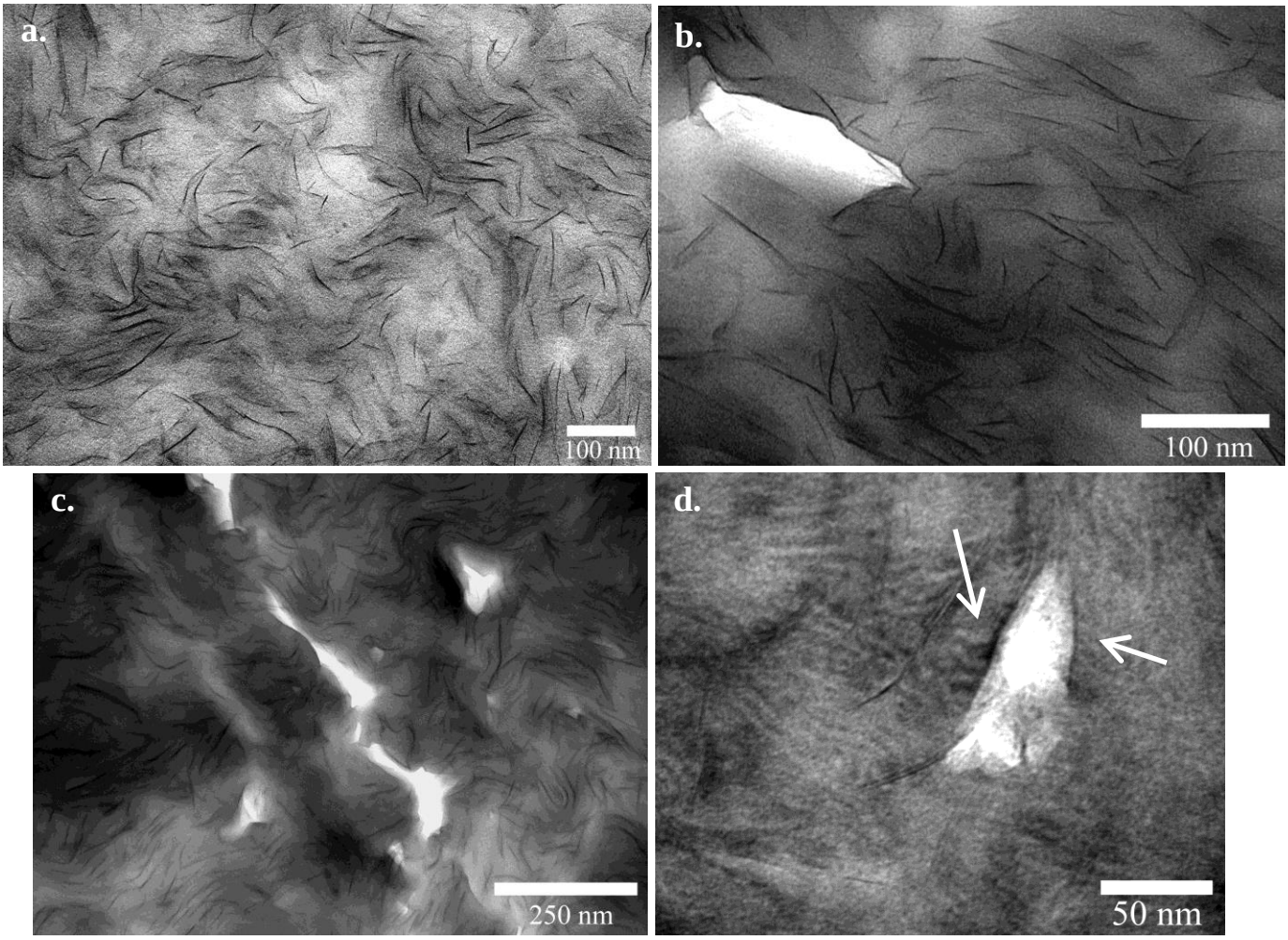

Figure 4. TEM micrographs in the core region of an injection molded exfoliated polyamide 6/organoclay nanocomposite (90/10) along a plane normal to the flow direction unloaded at different extensions showing (a) no debonding or delamination of clay layers; (b and c) formation of nano to submicron voids associated with delamination of clay layers; and (d) indicating the existence of trans-crystalline layers even after delamination.

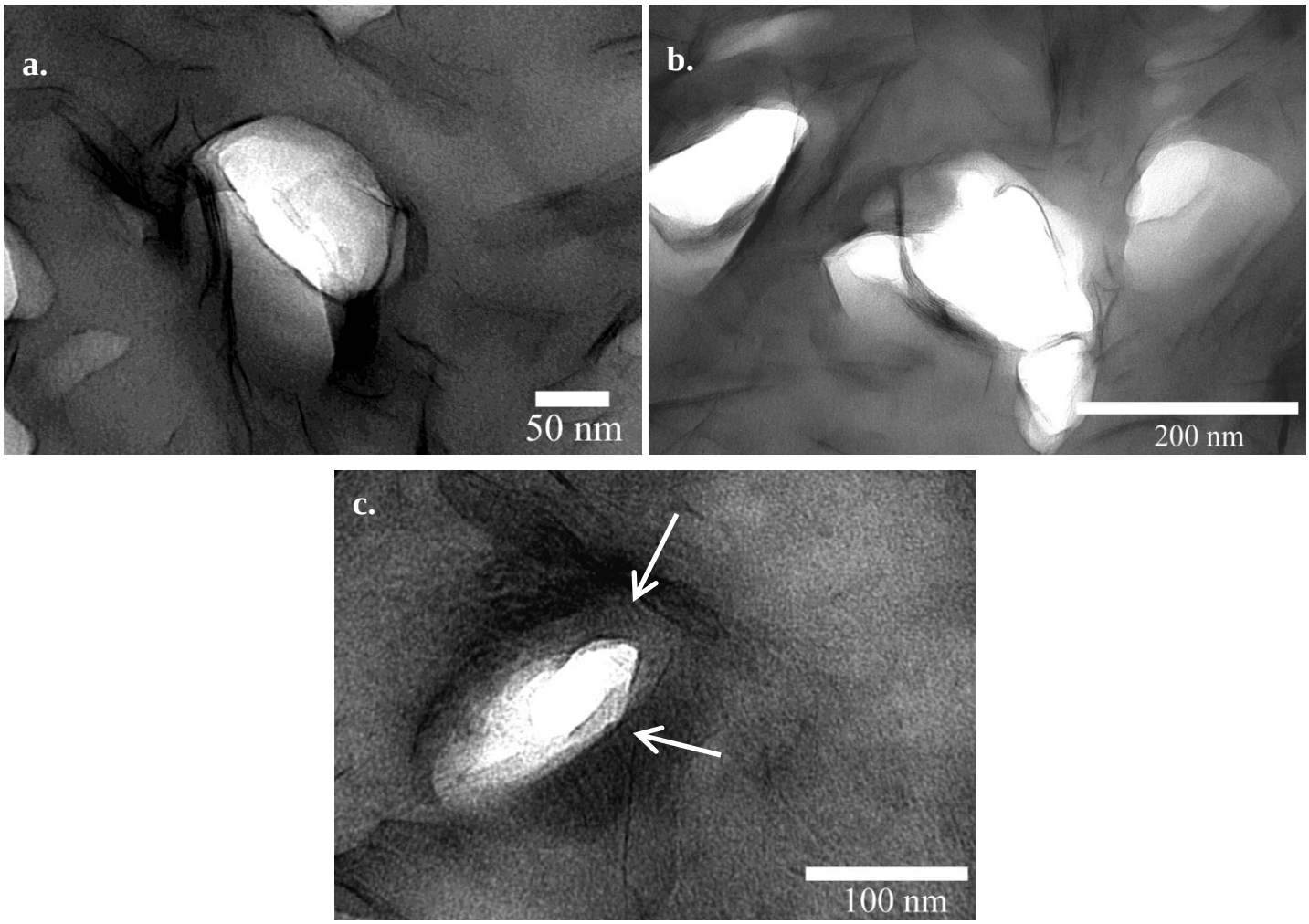

Figure 5. (a and b) TEM micrographs showing delamination of clay layers in tensile stretched intercalated polyamide 6/organoclay nanocomposite subjected to different extensions along with an example (c) indicating the existence of trans-crystalline layers even after delamination of clay layers.

This study adds to the basic information and understanding of the complexities involved in the crystalline organization in injection-molded polymer nanocomposites and points to the importance of accounting properly different effects of trans-crystalline regions on mechanical and physical properties of polymer nanocomposites.

Conclusions

- In the core region of injection molded polyamide 6/POE-g-MA blends, the presence of preferentially oriented lamellar zones around dispersed POE-g-MA particles of around 10-30 nm are observed. If the particles are intimately near each other, in the inter-particle regions of these particles, the crystalline lamellae are very

closely spaced. Near the surface regions, where the influence of shear exists, no preferentially oriented crystalline lamellae are found around the particles; and even when the inter-particle spacing is small, no crystalline lamellae are organized closely suggesting that flow-induced crystallization dominates at the surface regions.

- To identify the role of preferred lamellar organizations on the toughening processes, uniaxial tensile tests were performed. TEM observations of these tensile stretched samples showed that the orientation of the closely spaced lamellae along the tensile direction is a complex process and is dependent on the cavitation of POE-g-MA elastomeric particles to relieve the constraint on the matrix.
- Since the preferred oriented layers were only found in the core region of the injection molded bar and the toughness of the blend comprised deformation processes in all regions (surface, intermediate and core), it is concluded that the preferential alignment of lamellae in the vicinity of particles, particularly those closely-spaced lamellae in the inter-particle regions, may not be a predominant factor controlling the total toughness of the polymer blend.
- In the core region of injection molded polyamide 6/organoclay (90/10) nanocomposites, crystalline lamellae are normal to the lateral interfaces (both sides) of the clay layers and the matrix, and they are also closely organized. The trans-crystalline layers are around 30-40 nm (including both sides) for each clay layer. While in the near-surface regions, under the influence of shear-induced flow, flow-induced crystallization play a dominant role similar to the case of nylon 6/POE-g-MA blend.
- Delamination of clay layers was observed during tensile stretching in the polyamide 6/organoclay nano-composites, but no debonding of clay from the surrounding matrix was seen. Albeit delamination increases the toughness during the process of increasing the interlayer distance, it is thought that without extensive matrix shear yielding activated by full debonding of the clay/polymer matrix interfaces, large improvements in toughness cannot be realized.

Acknowledgements

We would like to thank the Australian Research Council (ARC) for the continuing support of this project on "Polymer Nanocomposites". YWM and ZZY are, respectively, Australian Federation Fellow and Australian Postdoctoral Fellow supported by the ARC and tenable at the University of Sydney. AD thanks the Australian Government for an International Postgraduate Research Scholarship Award and the University of Sydney for an International Postgraduate Award to undertake a PhD program in the CAMT. We also acknowledge the e-mail correspondence and discussions with Prof. L Leibler and Mr. L Corté of Ecole Supérieure de Physique Chimie Industrielle, France regarding staining of polyamide matrix and Ms. Cyn Lim for assistance in preparation of the studied materials.

References

1. Wang, K.H.; Chung, I.J.; Jang, M.C.; Keum, J.K.; Song, H.H. *Macromolecules* **2002**, *35*, 5529.
2. Kojima, Y.; Usuki, A.; Kawasumi, M.; Okada, A.; Kurauchi, T.; Kamigaito, O.; Kaji, K. *J. Polym. Sci. Part B: Polym. Phys.* **1995**, *33*, 1039.
3. Kim, G.M.; Lee, D.H.; Hoffman, B.; Kressler, J.; Stoppelmann, G. *Polymer* **2001**, *42*, 1095.
4. Corte, L.; Beaume, F.; Leibler, L. *Polymer* **2005**, *46*, 2748.
5. Muratoglu, O.K.; Argon, A.S.; Cohen, R.E.; Weinberg, M. *Polymer* **1995**, *36*, 921.
6. Kornfield, J.A.; Kumaraswamy, G.; Issaian, A.M. *Ind. Eng. Chem. Res*. **2002**, *41*, 6383.
7. Pearson, J.R.A. *Mechanics of Polymer Processing*, Elsevier: New York, **1988**.
8. Schultz, J.M. *Polymer Crystallization: The Development of Crystalline Order in Thermoplastics*, American Chemical Society, Oxford University Press, Washington, D.C., **2001**.
9. Zafeiropoulos, N.E.; Baillie, C.A.; Matthews, F.L. *Compos. Part A: Appl. Sci.* **2001**, *32*, 525.
10. Gassan, J; Mildner, I; Bledzki, A. *Compos. Interf.* **2001**, *8*, 443.
11. Arbelaiz, A.; Fernandez, B.; Ramos, J.A.; Mondragon, I. *Thermochim. Acta* **2006**, *440*, 111.

12. Chen, E.J.H.; Hsiao, B.S. *Polym. Engng. Sci.* **1992**, *32*, 280.

13. Thomason J.L.; Vanrooyen, A.A. *J. Mater. Sci.* **1992**, *27*, 897.

14. Varga, J.; Karger-Kocsis, J. *Polymer* **1995**, *36*, 4877.

15. Quan, H.; Li, Z.-M.; Yang, M.-B.; Huang, R. *Compos. Sci. Technol.* **2005**, *65*, 999.

16. Cho, K.; Kim, D.; Yoon, S. *Macromolecules* **2003**, *36*, 7652.

17. Andrews, E.H. *Proc. R. Soc. Lond. (A)* **1963**, *277*, 562.

18. Keller, A. *J. Polym. Sci.* **1959**, *35*, 361.

19. Bartczak, Z.; Argon, A.S.; Cohen, R.E.; Kowalewski, T. *Polymer* **1999**, *40*, 2367.

20. Sheng, N.; Boyce, M.C.; Parks, D.M.; Rutledge, G.C.; Abes, J.I.; Cohen, R.E. *Polymer* **2004**, *45*, 487.

21. Martinez-Salazar, J.; Cannon, C.G. *J. Mater. Sci. Lett.* **1984**, *3*, 693.

22. Lagasse, R.R.; Maxwell, B. *Polym. Engng. Sci.* **1976**, *16*, 189.

23. Keller, A. *J. Polym. Sci.* **1955**, *15*, 31.

24. Lazzeri, A.; Bucknall, C.B. *J. Mater. Sci.* **1993**, *28*, 6799.

25. Borggreve, R.J.M.; Gaymans, R.J.; Eichenwald, H.M. *Polymer* **1989**, *30*, 78.

26. Kinloch, A.J.; Shaw, S.J.; Tod, D.A.; Hunston, D.L. *Polymer* **1983**, *24*, 1341.

27. Usuki, A.; Kojima, Y.; Kawasumi, M.; Okada, A.; Fukushima, Y.; Kurauchi, T.; Kamigaito, O. *J. Mater. Res.* **1993**, *8*, 1179.

28. Shah, D.; Maiti, P.; Jiang, D.D.; Batt, C.A.; Giannelis, E.P. *Adv. Mater.* **2005**, *17*, 525.

29. Dasari, A.; Yu, Z.-Z.; Mai, Y.-W. *Acta Mater.* In press **2006**.